



HAL
open science

The second-degree gravity coefficients of Phobos from two Mars Express flybys

X Yang, J G Yan, T Andert, M Ye, M Pätzold, M Hahn, W T Jin, F Li,
Jean-Pierre Barriot

► **To cite this version:**

X Yang, J G Yan, T Andert, M Ye, M Pätzold, et al.. The second-degree gravity coefficients of Phobos from two Mars Express flybys. *Monthly Notices of the Royal Astronomical Society*, 2019, 490 (2), pp.2007-2012. 10.1093/mnras/stz2695 . hal-03155556

HAL Id: hal-03155556

<https://upf.hal.science/hal-03155556>

Submitted on 1 Mar 2021

HAL is a multi-disciplinary open access archive for the deposit and dissemination of scientific research documents, whether they are published or not. The documents may come from teaching and research institutions in France or abroad, or from public or private research centers.

L'archive ouverte pluridisciplinaire **HAL**, est destinée au dépôt et à la diffusion de documents scientifiques de niveau recherche, publiés ou non, émanant des établissements d'enseignement et de recherche français ou étrangers, des laboratoires publics ou privés.

The second-degree gravity coefficients of Phobos from two Mars Express flybys

X. Yang,^{1,2} J. G. Yan,^{1★} T. Andert,³ M. Ye,¹ M. Pätzold,⁴ M. Hahn,⁴ W. T. Jin,¹ F. Li¹
and J. P. Barriot^{1,5}

¹State Key Laboratory of Engineering in Surveying, Mapping and Remote Sensing, Wuhan University, 129 Luoyu Road, Wuhan 430070, China

²Royal Observatory of Belgium, 3 avenue Circulaire, B-1180 Uccle, Belgium

³Institute of Space Technology and Space Applications, Universität der Bundeswehr München, Neubiberg 85579, Germany

⁴Rheinisches Institut für Umweltforschung, Abteilung Planetenforschung, an der Universität zu Köln, Köln D-50931, Germany

⁵Observatoire Géodésique de Tahiti, University of French Polynesia, BP 6570, 98702 Faa'a, Tahiti, French Polynesia

Accepted 2019 September 19. Received 2019 September 13; in original form 2019 July 27

ABSTRACT

Several close spacecraft flybys of Phobos have been performed over the past 40 yr in order to determine the gravity field of this tiny Martian moon. In this work, the second-degree coefficients of the gravity field of Phobos were derived from the radio tracking data of two combined Mars Express flybys (2010 and 2013), by applying a least squares regularized inverse technique, that introduces as an *a priori* the gravity field retrieved from a shape model based on constant density hypothesis. A gravitational mass estimate of $(7.0765 \pm 0.0075) \times 10^5 \text{ m}^3 \text{ s}^{-2}$ and second-degree gravity coefficients $C_{20} = -0.1378 \pm 0.0348$ and $C_{22} = 0.0166 \pm 0.0153(3\sigma)$ were derived. The estimated C_{20} value, in contrast to the value of C_{20} computed from the shape model under the constant density assumption, supports an inhomogeneous distribution inside Phobos at a confidence interval of 95 per cent (1.96σ). This result indicates a denser mass in the equatorial region or lighter mass in polar areas.

Key words: methods: data analysis – planets and satellites: fundamental parameters – planets and satellites: interiors.

1 INTRODUCTION

The precise determination of the orbit of space probes and the perturbation of their motion is one of the best tools for estimating the gravity field of celestial bodies (Tapley, Schutz & Born 2004). Many spacecrafts have successfully flown over Phobos over the last 50 yr, in an effort to determine the mass of the tiny Martian moon (Christensen et al. 1977; Tolson et al. 1978; Williams, Duxbury & Hildebrand 1988; Kolyuka et al. 1990). The European Mars Express (MEX) spacecraft was one of those missions (Pätzold et al. 2014a).

The MEX flew by Phobos several times in the years 2006, 2008, 2010, and 2013 conducting radio science experiments at minimum distances of 460, 275, 77, and 59 km, respectively. Several estimates of the gravitational mass (GM; gravitational constant G times the mass M of the body) and second-degree gravity field coefficients from the analysis of the two-way Doppler recordings acquired during these flybys were published with increasing precision (Andert et al. 2010; Pätzold et al. 2014a, b). The latest estimate of the GM is

$(7.072 \pm 0.013) \times 10^5 \text{ m}^3 \text{ s}^{-2}$ (Pätzold et al. 2014b). The estimates of the second-degree and order gravity field coefficients, however, carry large error bars, which were linked to the signal-to-noise ratio, the uncertainty in the Phobos ephemeris and the geometries of the flybys (Yan et al. 2018).

Stable orbits around Phobos are not possible as the Hill sphere of Phobos lies inside the body, but quasi-synchronous orbits (QSO) are (Gil & Schwartz 2008; Matsumoto & Ikeda 2016). These QSO orbits can be described as an elliptical epicycles drifting back and forth in the direction of the orbital velocity of Phobos. They are named quasi-synchronous because they have revolution periods approximately equal to or multiples of the period of revolution of Phobos around Mars (Gil & Schwartz 2008). These orbits need to be maintained by frequent thruster firings (Matsumoto et al. 2018) which would perturb the motion of the spacecraft centre of mass (COM) and be an additional error source. Clearly, the determination of the Phobos gravity field from Doppler tracking at a degree and order higher than two is a challenging task.

The gravity field of Phobos is a powerful tool to constrain the internal structure of Phobos (Rosenblatt 2011), albeit the link between the internal density and the exterior gravity field is not unique. Phobos belongs to the family of small bodies, and it is

★ E-mail: jgyan@whu.edu.cn

probably made of a mix of undifferentiated chondritic material and maybe ice (Pang et al. 1978; Andert et al. 2010; Pätzold et al. 2014b). Two expected extreme variations of the internal structure could be: a homogeneous and highly porous body, or a re-accreted ‘rubble pile’ (Andert et al. 2010; Pätzold et al. 2014b). In this latter case, each block of the ‘rubble pile’ is probably homogeneous with no strong variations in density from block to block. Each block might be separated by small or large voids. It is believed that Phobos will be broken apart by tidal forces when or shortly before entering the Roche zone about Mars, and may crash on Mars in pieces in about 30 Myr from now (Efroimsky & Lainey 2007). The distinctive grooves on Phobos surface may be the signs of a global structural failure induced by these tidal forces (Hurford et al. 2016). Images also show that Phobos is blanketed by a regolith layer probably generated by the creation of the Stickney crater, but the depth of this blanket, probably less than some tens of meters, is still in debate (Wählisch et al. 2010).

In this paper, we will assume, as an *a priori*, that the gravity field of Phobos is not so different from the gravity field of a homogeneous body. This is simply because the available data (two data arcs) are not enough, in amount and noise level, to uniquely constrain by themselves the gravity field of Phobos. For this purpose, a sufficiently dense and precise coverage is needed, coverage that is of course not available to us currently. At this point, two possibilities are open: the first one, very conservative, is to stop here and to say that we need to wait for more data; the second one is to deal with the data we have at hand, and to complement them with sound *a priori* information. One of the simplest form of *a priori* information is to make the assumption that Phobos is reduced to a point mass, with only a central gravity field (i.e. with no higher gravity coefficients). This is done by adding, to the corresponding entries of the normal matrix, a small positive number, or a set of small positive numbers. This is widely used in terrestrial and planetary geodesy, under the name of Kaula’s spectral rule, and this was the choice applied by Pätzold et al. (2014b). This corresponds to look at gravity coefficients that are the closest possible to zero, or in other words, to look at a Phobos as ‘round as possible’, if we assume that its internal density is homogeneous. This is why we used in the previous lines the words ‘sound *a priori* information’, as we know from imaging that Phobos is not spherical. To assume a constant density is also a basic assumption, as there is no better replacement.

Therefore, as an *a priori* information, we used the gravity field from the Phobos shape model assuming a constant bulk density (a forward model), and we looked at second gravity coefficients that are not ‘so different’ from the ones computed from this model. As already said, this is certainly the best that can be done at this point with the data we have at hand. This type of forward model of the gravity field of Phobos was first derived by Davis, Housen & Greenberg (1981). In this paper we used as an *a priori* the second-degree and order coefficients from the model of Shi et al. (2012) computed from the shape model of Willner et al. (2010), with a constant density of 1.876kg m^{-3} (Andert et al. 2010). With this information, we processed two MEX flybys of 2010 and 2013, and retrieved new results of Phobos GM and second-degree gravity field coefficients. Indication of these results on Phobos interior structure was also studied. The paper is organized as follows: Section 2 presents methods and data we used for Phobos gravity field recovery. In Section 3, we made a choice of the optimum solution and gave a solution of Phobos GM and second-degree gravity field coefficients. The suggestion of Phobos interior from these results was also discussed in this section. Conclusions were drawn in Section 4.

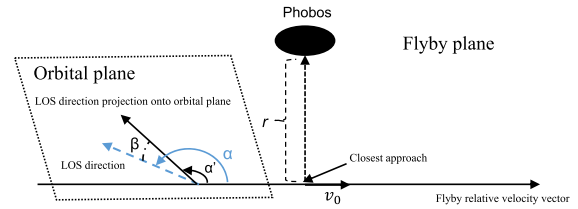


Figure 1. MEX flyby geometry at Phobos in 2010 and 2013. The flyby plane contains the flyby relative velocity v_0 and the position vectors from spacecraft to Phobos. The relative velocity v_0 forms an angle α with LOS direction and the LOS direction forms an angle β with the MEX orbital plane.

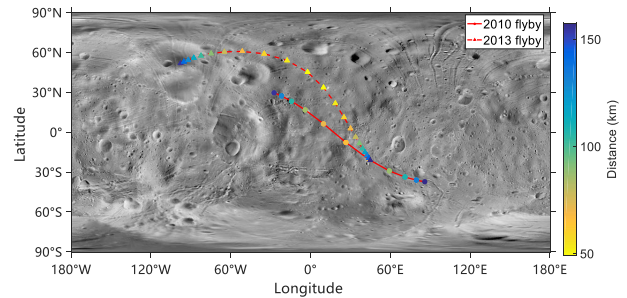


Figure 2. The ground track on Phobos surface of the two flybys. Considering the sensitivity of low-degree harmonics, only the points with a distance less than 150 km are plotted. The basemap is from Planetary Data System (Simonelli et al. 1993; Stooke 2012).

2 METHODS AND DATA

Phobos perturbs the motion of a spacecraft by its gravitational attraction during a close flyby. The magnitude of the Doppler shift caused by the Phobos attraction depends on the closest approach distance, the relative flyby velocity with respect to Phobos, the angle between trajectory and the direction to Earth and, of course, the GM of Phobos (Anderson 1971; Andert et al. 2010; Pätzold et al. 2014b; Yan et al. 2018). The highly elliptical orbit of MEX allows several flybys at Phobos, every five months, on average (Witasse et al. 2014; Pätzold et al. 2016), at distances from less than 100 km up to 2500 km. During the flyby of 2010 March, the Deep Space Network (DSN) tracked the MEX spacecraft by recording X-band and S-band carrier frequencies at its 70-m antenna near Madrid, Spain. The available tracking data consist of sets of data collected by the station in four-hour intervals, starting one hour before the closest approach of the spacecraft to Phobos until three hours after the closest approach. During the flyby of 2013 December, coherent two-way Doppler data were recorded at the 70-m antenna in Spain, at the 70-m antenna in California, and at the ESA 35-m antenna in Australia. About 30 h of Doppler tracking were recorded during this flyby, from 13 h before closest approach to 17 h after closest approach covering almost four full orbit periods of MEX about Mars.

The flyby geometry is shown in Fig. 1. The closest approach distances in 2010 and 2013 were 77 and 59 km, respectively. The relative velocities Phobos/MEX for the 2010 and 2013 flybys were both around 2.9 km s^{-1} ; the angles between the line of sight (LOS) and the MEX relative velocities were optimal at 82° and 85° ; the angles of the MEX orbit plane with respect to LOS were 10° and 6° , respectively. Both flyby geometries were optimal to solve for the Phobos gravity field (Yan et al. 2018). Fig. 2 shows the ground

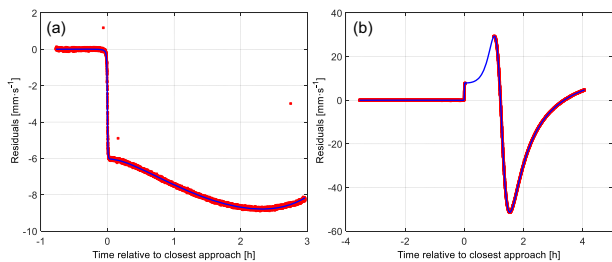


Figure 3. MEX Doppler velocity residuals (observed minus predicted without Phobos perturbation) from the (a) 2010 flyby and (b) 2013 flyby. The red dots represent the spacecraft Doppler velocity residuals with respect to the force model assuming that Phobos is not present. The blue line represents the least squares fit. The abrupt drop or raise in the relative velocity is caused by the gravity attraction of Phobos perturbing the motion of MEX, which occurs in less than one minute about closest approach. The gross error in data has been removed automatically. The orbital period of MEX is 6.5 h. A tracking gap occurred only minutes after closest approach in 2013 flyby due to an occultation of the spacecraft by Mars (missing red dots). The large amplitude Doppler shift after closest approach is caused by the pericentre passage of MEX. The post-encounter orbit of MEX is now perturbed and together with the high velocity through the pericentre results in larger post-encounter residuals compared to the unperturbed orbit.

track on Phobos surface of the two flybys with a distance between spacecraft and Phobos less than 150 km.

Our predicted Doppler velocity is based on a highly precise force model. The model includes the latest JPL Martian gravity field model (Konopliv, Park & Folkner 2016), the third-body perturbations from the Sun, and the large planets and large asteroids (Folkner et al. 2014). The post-Newtonian effect (Moyer 2005), the Mars solid tide perturbation (Konopliv et al. 2016), and the atmospheric drag (Forget et al. 1999) are also considered. The solar radiation pressure and thermal Martian albedo as well as indirect radiation (IR) were modelled as in Montenbruck & Gill (2012) and included in the prediction. The predicted values for the two-way Doppler were computed along with a precise knowledge of the ground station coordinates and tidal displacement (Mathews, Dehant & Gipson 1997). The state-of-the-art tropospheric correction model VMF1 were also incorporated during preprocessing (Boehm, Werl & Schuh 2006).

Fig. 3 shows the Doppler velocity residuals (observed minus predicted Doppler velocities without Phobos perturbation) during the MEX flybys of 2010 and 2013, respectively. A pre-encounter bias has been corrected by a baseline fit. A data gap during the 2013 flyby (fig. 3b) occurred because of the occultation of the spacecraft by Mars only minutes after closest approach (Pätzold et al. 2016).

The applied *a priori* gravity field of Phobos is calculated from the Phobos shape model of Willner et al. (2010) assuming a constant bulk density. The shape model is based on the IAU 2009 coordinate system and rotational elements (Archinal et al. 2011). The coordinate system has been revised recently in the IAU 2015 model (Archinal et al. 2018). In this paper therefore the Phobos coordinate system from the IAU 2015 model was used. Both IAU 2009 and IAU 2015 models are fully consistent at the level of 90 per cent concerning the orientation of the coordinate system at the time of the derivation of the shape model from MEX imaging (see supplementary material).

Inevitably, we expect a small deviation (around 10 m or less) between the COM of Phobos, implicitly used for the precise orbit determination (POD) software, and the IAU 2015 origin of the body frame (COF, or centre of figure). This implies the presence of small

non-zero first-degree coefficients in the forward model. However, we cannot jointly estimate the first-degree and the second-degree gravity field coefficients in the inverse model. This delicate point was treated in Yan et al. (2018). The main reason for this is that the ephemeris of Phobos is contaminated by errors that are at the same level, or larger, than the expected difference COM-COF. For example, the difference between the Phobos position from the ephemeris as reported by Jacobson (Jacobson & Lainey 2014) and Lainey (NOE-4-2015-b.bsp) was up to 233 m in the 2010 flyby and up to 216 m in the 2013 flyby. Hopefully, these numbers are small (2 per cent) with respect to the mean radius of Phobos, so even if the first-degree coefficients cannot be determined with accuracy, the orbital error will not undermine a safe determination of the higher degree and order coefficients. To be certain, we considered again the works of Shi et al. (2012) and added a shift in the X, Y, and Z directions to the facets of the polyhedron model of Phobos, and recomputed the gravity coefficients relative to the shifted models, for comparison with the original (unshifted) coefficients. Table 1 summarizes the results, and shows that the error induced by the orbital error in the determination of the second-degree coefficients is no larger than 0.52 per cent.

From a theoretical point of view, we should introduce in the POD software, as an add-on to the gravity field coefficients estimation, an estimation of the Phobos ephemeris error. As this ephemeris error cannot be separated with the estimation of first-degree coefficient and the gravity field of Phobos, we assumed, as an *a priori*, that they are zero. This is justified by the fact that the Doppler signal is, up to the first order, a mapping of velocity differences and not range differences, with a small error propagated into the gravity coefficients that are determined.

The coordinate frame of the Phobos shape model is also not perfectly aligned with the principal axes frame of the forward model (from the diagonalization of the inertia tensor). This explains the presence of the non-zero values, although small, of the C_{21} , S_{21} , and S_{22} coefficients in the forward model. In the inverse modelling, although the influence is subtle, it is not recommended to force the values to be zero, from a mathematical point of view, as the inverse least squares process will simply compensate by biasing the determination solution of the second-degree coefficients (Yan et al. 2018).

All calculations were performed with the software package MAGREAS developed at our laboratory in Wuhan, China (Yan et al. 2017; Ye et al. 2017). The detailed processing strategy and results can be found as online supplementary files of this paper.

3 RESULTS AND DISCUSSION

Table 2 shows the best estimate of the Phobos gravity field according to Section 2, taking into account the modelled gravity field of Phobos from the shape model as an *a priori* and the two-way Doppler velocity observations from the 2010 and 2013 MEX flybys. Three sets of *a priori* error bars are given for the second-degree and order gravity *a priori* coefficients. The first set, noted 200 per cent, means that the *a priori* error bars are equal to two times the values of the *a priori* gravity coefficients (solution A). The second set, noted 100 per cent, means that the *a priori* error bars are equal to the values of the *a priori* gravity coefficients (solution B). The third set, noted 50 per cent, means that the *a priori* error bars are equal to half the values of the *a priori* gravity coefficients (solution C). The *a priori* error bars of the GM coefficients is always (solutions A, B, and C) the *a posteriori* error bars of the solution from Pätzold et al. (2014a).

Table 1. The relative error of second-degree coefficients induced by the orbital error of Phobos. The axes mentioned below are in the Phobos body-fixed frame.

Relative error terms	Shift 200 m along X-axis (per cent)	Shift 200 m along Y-axis (per cent)	Shift 200 m along Z-axis (per cent)
C_{20}	0.16	0.16	0.31
C_{21}	0.00	0.00	0.00
S_{21}	0.00	0.00	0.00
C_{22}	0.52	0.52	0.00
S_{22}	0.00	0.00	0.00

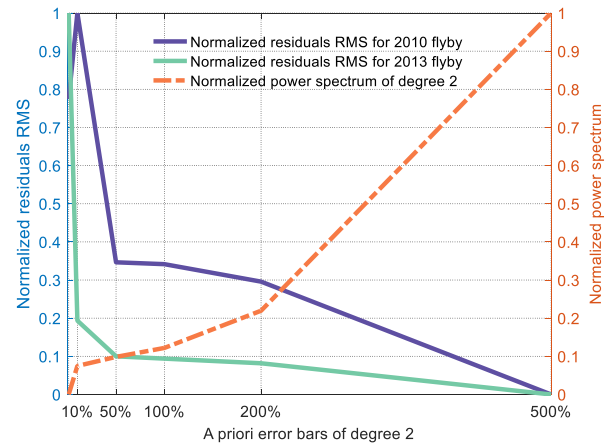
Table 2. Phobos gravity field derived from the MEX two-way Doppler residual velocities during the 2010 and 2013 flybys (not normalized coefficients). The *a priori* values of the second-degree and order gravitational coefficients correspond to the gravity field model computed from the shape model assuming constant density (see Section 1). The error of GM is adopted as $0.09 \times 10^5 \text{ m}^3 \text{ S}^{-2}$ (Pätzold et al. 2014a), and was fixed at that value for all runs. The reference radius of Phobos (10.993 km) was taken from the shape model (Willner, Shi & Oberst 2014). The uncertainties (1σ standard deviations) were derived from the diagonal of the inverse of the error matrix. The root-mean-squared residuals (RMS) in the table are the Doppler post-fit residuals.

Gravity field parameters	A priori values	Solution A (200 per cent level)		Solution B (100 per cent level)		Solution C (100 per cent level)	
		A priori error bars	Estimated values (1σ)	A priori error bars	Estimated values (1σ)	A priori error bars	Estimated values (1σ)
GM ($10^5 \text{ m}^3 \text{ s}^{-2}$)	7.1100	0.090	7.0764 ± 0.0028	0.090	7.0765 ± 0.0025	0.090	7.0765 ± 0.0020
C_{20}	-0.1073	0.2146	-0.1389 ± 0.0132	0.1073	-0.1378 ± 0.0116	0.0537	-0.1375 ± 0.0089
C_{21}	0.0018	0.0036	0.0031 ± 0.0025	0.0018	0.0025 ± 0.0013	0.0009	0.0024 ± 0.00063
C_{22}	0.0161	0.0322	0.0164 ± 0.0057	0.0161	0.0166 ± 0.0051	0.0080	0.0166 ± 0.0040
S_{21}	-0.00077	0.0015	-0.00078 ± 0.0011	0.00077	-0.00078 ± 0.00054	0.00038	-0.00077 ± 0.00027
S_{22}	0.00041	0.00082	0.00068 ± 0.00058	0.00041	0.00057 ± 0.00029	0.00020	0.00054 ± 0.00015
Residuals RMS for 2010 flyby (mm s^{-1})			0.04104819		0.04104953		0.04104967
Residuals RMS for 2013 flyby (mm s^{-1})			0.08348612		0.08348669		0.08348697
Residuals whole RMS (mm s^{-1})			0.07933498		0.07933570		0.07933587

The MEX spacecraft was tracked by the 70-m DSN antenna and the ESA 35-m antenna during the 2013 flyby (while only the 70 m antenna was used for the 2010 flyby), and the line-of-sight Earth–Mars was closer to the Sun than during the 2010 flyby. The radio signal propagated deeper through the coronal plasma than in 2010 and induced a higher plasma noise on the carrier frequency (Pätzold et al. 2016). This explains the higher noise level of the Doppler velocity residuals for the 2013 flyby compared to the 2010 flyby.

The norm of the residuals is at the maximum value when the error bars for the *a priori* model were set to zero. This means that the *a posteriori* gravity model is the same as the *a priori* model of Shi et al. (2012). If we push the *a priori* error bars up to infinite (i.e. very large) values, then the *a posteriori* gravity model is free to take the values that realize the minimum of the Doppler residuals. In our case, strictly speaking, the quantity that is minimized (a total fit) is the Doppler data fit and, altogether, the fit to the gravity *a priori* model with a to-be-determined weight between them. This procedure, called Morozov’s discrepancy principle (Morozov 1984), is standard in inverse problems with *a priori* information and outlined in Barriot & Balmino (1992) for space geodesy applications. The best fit of the Doppler data, in this sense, makes a compromise between the RMS residuals and the power spectrum at second degree. Fig. 4 shows our choice of the *a priori* error bars. The *X*-axis of the cross point of 2013 flyby, which falls in the areas between 50 per cent and 100 per cent level, corresponds to the best *a priori* error bar for the second-degree harmonics, which is because the flyby in 2013 has longer tracking time (30 h versus 4 h) and shorter closest approach (59 km versus 77 km). We retained the 100 per cent error bar in our final estimate, but the 50 per cent and 200 per cent choices yielded close estimates.

The estimates of the Phobos GM determined from several space missions over the past 40 yr are presented in Fig. 5. The differences are explained by frequency noise, choice of tracking frequency,

**Figure 4.** Choice of the optimum solution. The *X*-axis is the percentage of the *a priori* error bar, the left *Y*-axis the normalized Doppler residuals, and the right *Y*-axis the normalized power spectrum of second degree. From the figure, it is clear that the best compromise between the post-fit Doppler residuals and the power spectrum of the second-degree coefficients is realized for second-degree coefficients priori error bars in the range of 50 per cent to 200 per cent (see Table 2 for the *a priori* values and error bars). The corresponding *a posteriori* values are plotted in Fig. 6.

knowledge of spacecraft and Phobos orbit and its precision, flyby geometry and many more. Lainey, Dehant & Pätzold (2007) were the first to adopt a full numerical integration to derive the ephemeris of Phobos. Before that, the Phobos ephemeris was derived by adjusting an analytical time series with free parameters (Morley 1990). Therefore, looking at the GM estimates after 2007, we could see that the estimates are quite consistent. A rough trend could be seen from Fig. 5 that the GM estimates are getting lower values. The reason of lower GM value we obtained in this work is

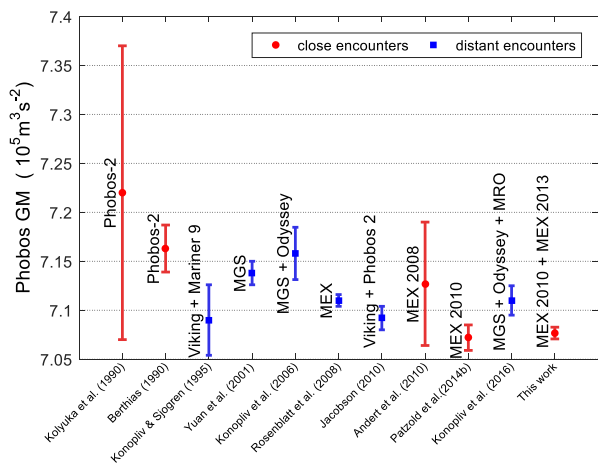


Figure 5. Phobos GM solutions from close and distant encounters. These values are from the relevant publications (cited on each horizontal axis label) and the error bars are set to 3σ for comparison (Berthias 1990; Kolyuka et al. 1990; Konopliv & Sjogren 1995; Yuan et al. 2001; Konopliv et al. 2006; Rosenblatt et al. 2008; Andert et al. 2010; Jacobson 2010; Pätzold et al. 2014b; Konopliv et al. 2016). The GM value we reported here is $(7.0765 \pm 0.0075) \times 10^5 \text{ m}^3 \text{ s}^{-2}$.

probably that the second-degree harmonics and GM are estimated at the same time, while others were not, except Pätzold et al. (2014b), which is consistent with us. Our estimate of the mass M of Phobos is computed to be $(1.0604 \pm 0.0011) \times 10^{16} \text{ kg}$ [for $G = (6.67408 \pm 0.00031) \times 10^{-11} \text{ m}^3 \text{ kg}^{-1} \text{ s}^{-2}$]. The volume of the shape model is $5742 \pm 35 \text{ km}^3$ (Willner et al. 2014) which yields a bulk density of $(1846 \pm 11) \text{ kg m}^{-3}$. As already stated by Andert et al. (2010), Rosenblatt (2011), and Pätzold et al. (2014a), this low bulk density implies that the interior of Phobos must be porous.

At the time of this writing, Pätzold et al. (2014b) and Jacobson & Lainey (2014) estimated the C_{20} and C_{22} coefficients. The estimation by Pätzold et al. (2014b) is based on the Doppler data from the MEX 2010 flyby, and this may explain the large error bar on the C_{20} estimate. The estimation from Jacobson & Lainey (2014) with a concomitant estimation of the ephemeris of Phobos was based on Earth-based optical data and spacecraft Doppler/optical data collected from 1877 to 2007. Jacobson & Lainey (2014) adopted the libration amplitude based on the homogeneous hypothesis and did not estimate libration. They emphasized that they were not fully able to separate the libration parameters of Phobos with respect to the C_{20} and C_{22} coefficients, which meant that the coefficients will change if Phobos is inhomogeneous. Otherwise, our estimates are consistent within the errors with the values given by these two authors.

The second-degree and order gravity coefficients provide a way to constrain the inertia tensor of a body; albeit this constraint is not complete, as the inertia tensor is characterized by six independent values and there are only five second-degree and order coefficients. The full inertia tensor can only be derived by adding information about the rotational state of the body. The libration in longitude of Phobos carries such information (Matsumoto & Ikeda 2016). Matsumoto & Ikeda (2016) claim that a few per cent in accuracy (with respect to the true, unknown value) for the degree and order two coefficients is needed to model a possible heterogeneity in the interior of Phobos. In this respect, the error of the C_{20} coefficient derived by Pätzold et al. (2014b) is too large. We believe that our

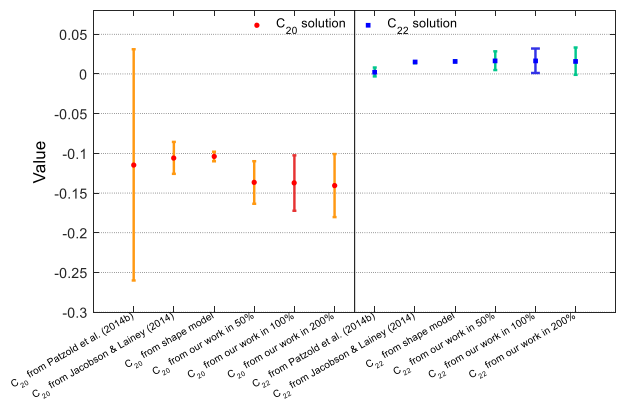


Figure 6. Comparison of the Phobos C_{20} and C_{22} gravity coefficients estimates from different authors (X -axis), including this work. The percentage values (50 per cent, 100 per cent, and 200 per cent) represent the *a priori* error bars added during the calculation. All post-fit error bars are 3σ . The harmonic coefficients are not normalized with a reference radius of 10.993 km. The C_{20} and C_{22} computed from the shape model are -0.1072 ± 0.006 and 0.0161 ± 0.0012 , respectively. The best fits from this work are $C_{20} = -0.1378 \pm 0.0348$ and $C_{22} = 0.0166 \pm 0.0153$.

estimates, as computed in this paper, meet the basic requirements for interpreting the interior of Phobos.

The C_{20} value from the shape model with constant density shall be used as a reference value to interpret the Phobos internal mass distribution (Pätzold et al. 2014b; Le Maistre, Rivoldini & Rosenblatt 2019). From Fig. 6, our measured value of C_{20} is mostly lower than the C_{20} value from shape, which is statistically inconsistent with a homogeneous and uniform distribution inside Phobos within the confidence interval of 95 per cent. The value of C_{20} is also related to the moments of inertia (MoI) of Phobos by:

$$C_{20} = \frac{A + B}{2} - C \quad (1)$$

where A, B, and C are normalized MoI along the principle axes of x , y , and z . From equation (1), the lower estimate of C_{20} suggests lower equatorial moment of inertia or larger polar moment of inertia, indicating a denser mass in the equatorial region or lighter mass in polar areas with respect to Phobos bulk density.

4 CONCLUSIONS

In this work, we estimated the Phobos gravitational parameter GM, and the C_{20} , and C_{22} gravity coefficients from the MEX 2010 and 2013 Phobos flybys using the latest orientation of the Phobos coordinate system (IAU 2015). We introduced *a priori* values for the gravity inverse problem, computed from a shape model assuming a constant density (Shi et al. 2012). Our best estimate for GM is $(7.0765 \pm 0.0075) \times 10^5 \text{ m}^3 \text{ s}^{-2} (3\sigma)$, leading to a bulk density of Phobos of $(1846 \pm 11) \text{ kg m}^{-3}$ using the volume of the shape model of $(5742 \pm 35) \text{ km}^3$.

Our best estimates for the second-degree and order coefficients are $C_{20} = -0.1378 \pm 0.0348(3\sigma)$ and $C_{22} = 0.0166 \pm 0.0153(3\sigma)$. The value of C_{20} , mostly lower than the theoretical C_{20} from the shape model with constant density, suggests an inhomogeneous distribution inside Phobos, implying a denser mass in the equatorial region or lighter mass in polar areas.

ACKNOWLEDGEMENTS

We are grateful to NASA and ESA for providing models to make this research possible. This work could not have been successful without the efforts of the ESA Mars Express Science Operations teams, the MEX Flight Control Team, and the ESA ESTRACK and NASA Deep Space Network ground station crews. The data used in this paper are available at <ftp://psa.esac.esa.int>. Richard Simpson and B. Häusler involved in data acquisition and validation. XY thanks Dr. Sebastien Le Maistre for his insightful comments and advice. This work is supported by National Scientific Foundation of China (U1831132, 41874010, 41804025), Innovation Group of Natural Fund of Hubei Province (2018CFA087), and China Postdoctoral Science Foundation (2016M602360). The Open Funding of Macau University of Science and Technology (FDCT 119/2017/A3) also supports this work. XY and WTJ are sponsored by the China Scholarship Council. TA is funded by the German Space Agency (DLR) under the grant 50QM1704. JPB is funded by a DAR grant in planetology from the French Space Agency (CNES). MP and MH are funded by the Bundesministerium für Wirtschaft und Energie, Berlin, via the German Space Agency DLR, Bonn, under grant 50QM1802.

REFERENCES

- Anderson J. D., 1971, in International Astronomical Union Colloquium, Cambridge University Press, Cambridge, p. 577
- Andert T. P., Rosenblatt P., Pätzold M., Häusler B., Dehant V., Tyler G. L., Marty J. C., 2010, *Geophys. Res. Lett.*, 37, L09202
- Archinal B. A. et al., 2018, *Celest. Mech. Dyn. Astron.*, 130, 22
- Archinal B. A. et al., 2011, *Celest. Mech. Dyn. Astron.*, 109, 101
- Barriot J. P., Balmino G., 1992, *Icarus*, 99, 202
- Berthias J., 1990, Jet Propulsion Laboratory. California Institute of Technology, Pasadena, CA
- Boehm J., Werl B., Schuh H., 2006, *J. Geophys. Res.*, 111, B02406
- Christensen E. J., Born G. H., Hildebrand C. E., Williams B. G., 1977, *Geophys. Res. Lett.*, 4, 555
- Davis D. R., Housen K. R., Greenberg R., 1981, *Icarus*, 47, 220
- Efroimsky M., Lainey V., 2007, *J. Geophys. Res.*, 112, E12003
- Folkner W. M., Williams J. G., Boggs D. H., Park R. S., Kuchynka P., 2014, Interplanetary Network Progress Report, 196, 1
- Forget F. et al., 1999, *J. Geophys. Res.*, 104, 24155
- Gil P., Schwartz J., 2008, in AIAA/AAS Astrodynamics Specialist Conference and Exhibit, Aerospace Research Central, Honolulu, Hawaii, p. 6429
- Hurford T. et al., 2016, *J. Geophys. Res.*, 121, 1054
- Jacobson R. A., 2010, *AJ*, 139, 668
- Jacobson R. A., Lainey V., 2014, *Planet. Space Sci.*, 102, 35
- Kolyuka Y. F., Efimov A. E., Kudryavtsev S. M., Margorin O. K., Tarasov V. P., Tikhonov V. F., 1990, *SvA*, 16, 168
- Konopliv A., Sjogren W., 1995, JPL technical Reports, Lab., Calif. Inst. of Technol., Pasadena
- Konopliv A. S., Yoder C. F., Standish E. M., Yuan D.-N., Sjogren W. L., 2006, *Icarus*, 182, 23
- Konopliv A. S., Park R. S., Folkner W. M., 2016, *Icarus*, 274, 253
- Lainey V., Dehant V., Pätzold M., 2007, *A&A*, 465, 1075
- Le Maistre S., Rivoldini A., Rosenblatt P., 2019, *Icarus*, 321, 272
- Mathews P. M., Dehant V., Gipson J. M., 1997, *J. Geophys. Res.*, 102, 20469
- Matsumoto K., Ikeda H., 2016, in Lunar and Planetary Science Conference, SAO/NASA Astrophysics Data System, p. 1846

- Matsumoto K., Ikeda H., Hirata N., Kouyama T., Senshu H., Araya A., 2018, in Symposium on Asteroids and Comet Gravity and Interiors. Wuhan University, Wuhan, China
- Montenbruck O., Gill E., 2012, *Satellite Orbits: Models, Methods and Applications*. Springer Science & Business Media, Berlin Heidelberg 2000,
- Morley T. A., 1990, *A&A*, 228, 260
- Morozov V. A., 1984, *The Regularization Method. in Methods for Solving Incorrectly Posed Problems*. Springer, New York, NY
- Moyer T. D., 2005, *Formulation for Observed and Computed Values of Deep Space Network Data Types for Navigation*. Vol. 3, John Wiley & Sons, Hoboken, New Jersey
- Pang K. D., Pollack J. B., Veverka J., Lane A. L., Ajello J. M., 1978, *Science*, 199, 64
- Pätzold M., Andert T., Jacobson R., Rosenblatt P., Dehant V., 2014a, *Planet. Space Sci.*, 102, 86
- Pätzold M., Andert T., Tyler G., Asmar S., Häusler B., Tellmann S., 2014b, *Icarus*, 229, 92
- Pätzold M. et al., 2016, *Planet. Space Sci.*, 127, 44
- Rosenblatt P., 2011, *A&AR*, 19, 44
- Rosenblatt P., Lainey V., Le Maistre S., Marty J. C., Dehant V., Pätzold M., Van Hoolst T., Häusler B., 2008, *Planet. Space Sci.*, 56, 1043
- Shi X., Willner K., Oberst J., Ping J., Ye S., 2012, *Sci. China Phys., Mech. Astron.*, 55, 358
- Simonelli D. P., Thomas P. C., Carcich B. T., Veverka J., 1993, *Icarus*, 103, 49
- Stooke P., 2012, *Stooke Small Bodies Maps V2.0. MULTI-SA-MULTI-6-STOOKEMAPS-V2.0*, NASA Planetary Data System
- Tapley B., Schutz B., Born G. H., 2004, *Statistical Orbit Determination*. Elsevier, Burlington, USA
- Tolson R. H. et al., 1978, *Science*, 199, 61
- Wählisch M. et al., 2010, *Earth Planet. Sci. Lett.*, 294, 547
- Williams B., Duxbury T., Hildebrand C., 1988, in Lunar and Planetary Science Conference, JPL, California Institute of Technology, Pasadena, CA
- Willner K., Oberst J., Hussmann H., Giese B., Hoffmann H., Matz K.-D., Roatsch T., Duxbury T., 2010, *Earth Planet. Sci. Lett.*, 294, 541
- Willner K., Shi X., Oberst J., 2014, *Planet. Space Sci.*, 102, 51
- Witasse O. et al., 2014, *Planet. Space Sci.*, 102, 18
- Yan J., Yang X., Ye M., Li F., Jin W., Barriot J.-P., 2017, *Astrophys. Space Sci.*, 362, 123
- Yan J. G., Yang X., Ye M., Andert T., Jin W. T., Li F., Jin S. G., Barriot J. P., 2018, *MNRAS*, 481, 4361
- Ye M., Li F., Yan J., Hao W., Yang X., Jin W., Qu C., 2017, *Cehui Xuebao/Acta Geodaetica et Cartographica Sinica*, 46, 288
- Yuan D.-N., Sjogren W. L., Konopliv A. S., Kucinskis A. B., 2001, *J. Geophys. Res.*, 106, 23377

SUPPORTING INFORMATION

Supplementary data are available at [MNRAS](https://www.mnras.org) online.

Appendix

Please note: Oxford University Press is not responsible for the content or functionality of any supporting materials supplied by the authors. Any queries (other than missing material) should be directed to the corresponding author for the article.

This paper has been typeset from a $\text{\TeX}/\text{\LaTeX}$ file prepared by the author.